International Journal of Secondary Metabolite
2022, Vol. 9, No. 2, 208–228
https://doi.org/10.21448/ijsm.1023864
Published at https://dergipark.org.tr/en/pub/ijsm
Research Article

Molecular Docking, Antibacterial and Antioxidant Activities of Compounds Isolated from Ethiopian Plants

Yadessa Melaku[1,*], **Tokuma Getahun**[1], **Markos Addisu**[1], **Hailemichael Tesso**[1], **Rajalakshmanan Eswaramoorthy**[1], **Ankita Garg**[1]

[1]Chemistry Department, School of Applied Natural Sciences, Adama Science and Technology University, P.O.Box 1888, Adama, Ethiopia

Abstract: This study evaluated the antibacterial and antioxidant activities of the constituents of *L. tomentosa* and *S. longipedunculata*. The *in-silico* molecular docking analysis of the isolated compounds was also reported herein for the first time. The GC-MS analysis of the essential oil of *L. tomentosa* led to the identification of eleven components with 2,5-dimethoxy-*p*-cymene identified as the principal constituent (59.39%). Lauric acid (**1**), *β*-stigmasterol (**2**), chrysophanol (**3**), and emodin (**4**) were isolated from *L. tomentosa* using silica gel column chromatography. Likewise, 9H-xanthene-3,5-diol (**5**), 1,7-dihydroxy-4-methoxyxanthone (**6**), and oleic acid (**7**) were isolated from *S. longipedunculata*. The structures of the isolated compounds were elucidated using UV-Vis, IR, and NMR spectroscopic methods. Compounds **3** and **4** are new to the genus Laggera, while **5** and **6** are new to the species *S. longipedunculata*. Compounds **3-6** inhibited DPPH radical by 86, 92, 88, and 90%, respectively. Compounds **5** and **6** inhibited 79.2 and 81.9% peroxide formation, respectively. The antioxidant activities displayed by compounds **4-6** suggest their use as a natural antioxidant. Compounds **4** and **6** inhibited the growth of bacteria by 18.00±0.10 and 16.06±0.22 mm, respectively. Compounds **3**, **4**, and **6** showed binding affinities of −10.4, −10.4, and −9.9 kcal/mol against *Staphylococcus aureus* DNA Gyrase, respectively, while **4** showed −10.4 kcal/mol against human topoisomerase IIβ. Therefore, the present study results showed that emodin and 1,7-dihydroxy-4-methoxyxanthone might be considered lead compounds for further development as antibacterial and anti-cancer agents. The findings also substantiate the traditional use of these plants against bacteria.

ARTICLE HISTORY
Received: Nov. 15, 2021
Revised: Feb. 12, 2022
Accepted: May 10, 2022

KEYWORDS
L. tomentosa,
S. longipedunculata,
Phytochemicals,
Antibacterial,
Antioxidant.

1. INTRODUCTION

Laggera tomentosa (Asteraceae) is a perennial plant endemic to Ethiopia growing in Shewa, Arsi, Wollo, Gonder and Gojjam (Asfaw, Storesund, Aasen, & Skattebol, 2003). The plant is traditionally used in Ethiopia against tooth-ache, stomach-ache, swellings, ringworm, and infections. The compounds 2,4,4-trimethylbicyclo[3.1.1]hept-2-en-6-one, 2,7,7-

*CONTACT: Yadessa Melaku ✉ yadessamelaku2010@gmail.com Chemistry Department, School of Applied Natural Sciences, Adama Science and Technology University, P.O.Box 1888, Adama, Ethiopia

ISSN-e: 2148-6905 / **© IJSM 2022**

trimethylbicyclo[3.1.1]hept-2-en-6-one, (2E,4E)-3,7-dimethylocta-2,4,6-trienal, (2Z,4E)-3,7-dimethylocta-2,4,6-trienal, 1,4-dimethoxy-5-methyl-2-(1-methylethyl)benzene have been reported from the essential oil of the leaves of *L. tomentosa* (Asfaw, Storesund, Aasen, & Skattebol, 2003). Furthermore, the leaves were reported to be rich in flavonoids including 4-*O*-acetylcuauthemone-3-*O*-(2'-hydroxy-2'-methyl-3'-acetoxybutyrate), 3-*O*-(3'-acetoxy-2'-hydroxy-2'-methylbutyryl)cuauthemone, 4-*O*-acetylcuauthemone-3-*O*-angelate, 3',5,6-trihydroxy-3,4',7-trimethoxyflavone, 3',4',5,7-tetrahydroxy-3,6-dimethoxyflavone, 4',5,7-trihydroxy-3',3,6-trimethoxyflavone, 3',5,7-trihydroxy-3,4',6-trimethoxyflavone (Kibrom, Dibaba, & Nigist, 2010).

Securidaca longipedunculata (Polygalaceae) is a popular hedge plant in Ethiopia traditionally used for washing clothes because of its foam-forming ability in the water. The plant is also used to treat arthritis, wounds, cough, venereal diseases, tuberculosis, and skin diseases (Debella *et al*., 2000) (Dibwe *et al*., 2013). Previous pharmacological reporting has shown that the extracts exhibit anti-inflammatory activity (Akpemi *et al*., 2013). Chemically, *S. longipedunculata* was reported to have quercetin-3-*O*-D-xyloside (Debella *et al*., 2000), benzyl-6-methoxybenzoate, cinnamic acid, caffeic acid, cinapic acid, *p*-coumaric acid and *β*-sitosterol (Mongalo *et al*., 2015). Though these plants are traditionally used to treat a wide array of diseases, there is no report on the isolation of compounds responsible for the antibacterial and antioxidant activities of the extracts of *L. tomentosa* and *S. longipedunculata*. Therefore, this paper presents the study results on the chemical constituents, antibacterial and radical scavenging activities of the root extracts of *L. tomentosa*, and stem barks of *S. longipedunculata*. Also incorporated herein are the reports on the *in-silico* molecular docking, ADMET, and DFT analysis of compounds isolated from *L. tomentosa* and *S. longipedunculata*.

2. MATERIAL and METHODS

2.1. Plant Material

L. tomentosa and *S. longipedunculata* were collected in November 2018 from Sebeta and Menesibu, Ethiopia, respectively. A botanist identified the plants, and voucher specimens GW003 for *L. tomentosa* and M002 for *S. longipedunculata* were deposited at the National Herbarium of Addis Ababa University, Ethiopia.

2.2. Extraction and Isolation

2.2.1. *Roots of laggera tomentosa*

The root of *L. tomentosa* (300 g) was successively extracted with each 1.2 L of *n*-hexane, EtOAc, and MeOH using maceration for 72 hrs. Each extract was filtered and concentrated by a rotary evaporator at 40^{o}C to afford 3.22, 5.06, and 6.88 g, respectively. The EtOAc extract (4.06 g) was fractionated over silica gel (160 g) column chromatography using *n*-hexane: EtOAc: MeOH as eluent to give ten fractions, each 300 mL. Fractions 1, 2, 3, 4 and 5 were eluted using *n*-hexane: EtOAc 9:1, 7:3, 3:2, 3:7 and 1:9, respectively. Fraction 6 was eluted with 100% EtOAc. Fractions 7, 8, 9 and 10 were eluted with EtOAc: MeOH in 9:1, 8:2, 7:3 and 1:1, respectively. Fractions eluted with *n*-hexane: EtOAc (7:3) after silica gel column chromatography gave compound **1** (19 mg) while compounds **2** (21 mg) and **3** (9 mg) were isolated from the fraction eluted with *n*-hexane: EtOAc (3:7). Fraction 7 was fractionated over silica gel column chromatography using *n*-hexane: EtOAc (1:9) to afford six fractions, 25 mL each. Sub-fraction 3 was found to be compound **4** (13 mg).

2.2.2. *Stem barks of securidaca longipedunculata*

The stem bark of *S. longipedunculata* (500 g) was successively extracted using maceration using *n*-hexane, EtOAc, and MeOH, each 2.5 L for 72 hrs. A rotary evaporator filtered and concentrated the extracts at 40^{o}C to give 2.6, 5, and 51 g. The EtOAc extract (5 g) was subjected

to silica gel (150 g) column chromatography using the increasing polarity of EtOAc in *n*-hexane as eluent to afford 40 fractions, each 100 mL. The First 1-5 were eluted with *n*-hexane. The next three fractions were eluted with *n*-hexane: EtOAc (9:1). Fractions 9-11 were eluted with *n*-hexane:EtOAc (4:1). Fraction 12-14, Fraction 15-17, Fraction 18-21, Fraction 22-24, Fraction 25-27, Fraction 28-30, Fraction 31-34 were collected using *n*-hexane:EtOAc (7:3), *n*-hexane:EtOAc (6:4), *n*-hexane:EtOAc (1:1), *n*-hexane:EtOAc (4:6), *n*-hexane:EtOAc (3:7), *n*-hexane:EtOAc (1:4) and *n*-hexane:EtOAc (1:9), respectively. The last six fractions were collected using EtOAc. Fraction 15-18, eluted with *n*-hexane: EtOAc (3:2), was identified as compound **5** (17 mg) as yellow crystals. Fraction 18-21, eluted with *n*-hexane: EtOAc (1:1), was identified as compound **6** (8 mg). Fractions eluted with *n*-hexane: EtOAc (3:7) after silica gel column chromatography gave compound **7** (7 mg) as a white solid.

2.3. GC-MS analysis of *n*-hexane extract of the roots of *L. Tomentosa*

The essential oil obtained from the *n*-hexane extract of *L. tomentosa* was analyzed using Agilent Technologies 7820A GC system with Agilent technologies 5977E mass selective detector, USA.

2.4. Antioxidant Activity

2.4.1. *Radical scavenging activity*

The radical scavenging activity of the samples was evaluated using DPPH as described in the previously reported protocol (Brand-Williams, Cuvelier, & Berset, 1995). The standard solution (500 μg/mL) was prepared by dissolving each sample in MeOH. Each solution was serially diluted in 0.1 mM DPPH in MeOH to give 100, 50, 25, and 12.5 μg/mL. After an incubation period of 30 minutes at 37°C, the absorbance of the sample was measured at 517 nm using a UV-Vis spectrophotometer (Ghasemi *et al*., 2009). This measurement was repeated for ascorbic acid. The experiments were performed in triplicates and reported as M±SD. The % radical scavenging activity was then calculated with the following formula (Qusti *et al*., 2010):

$$\% \text{ Inhibition} = \frac{(A_{control} - A_{extract})}{A_{control}} \times 100$$

Where $A_{control}$ is the absorbance of DPPH solution and $A_{extract}$ is the absorbance of the test sample (DPPH solution plus sample)

2.4.2. *Ferric thiocyanate method*

The ferric thiocyanate method was used to assess the anti-lipid peroxidation potential of the samples following the previously reported procedure (Nagatsu, 2004). Each sample (0.1 mg), linoleic acid (100 µL), EtOH (5 mL), and phosphate buffer (5 mL, 0.05 M, pH = 7) in water were added into a vial and then incubated for 24 h at 40°C. An aliquot (0.1 mL) was taken and added into a vial containing 75% aqueous ethanol (7 mL), 30% of NH_4SCN (0.15 mL) and 0.15 mL of 0.02M $FeCl_2$ in 3.5% HCl. The samples were then subjected to a UV-Vis spectrophotometer to measure the absorbance at 500 nm. This measurement was repeated for the blank and ascorbic acid. The % inhibition is calculated using the following formula (Gülçin *et al*., 2010).

$$Percentage\ inhibition = 100 - \left(\frac{As}{Ab} x100\right)\%$$

Where As is absorbance of the sample and Ab is absorbance of the blank.

2.5. Antibacterial Activities

The samples were evaluated for their *in-vitro* antibacterial activity using the disc diffusion method against *E. coli* (ATCC25922), *P. mirabilis* (ATCC 35659), *K. pneumoniae*

(ATCC700603), *S. typhi* (ATCC1331), *S. aureus*, (ATCC25923) and *B. subtilis* (ATCC6633) (Ołdak *et al*., 2017). The bacterial species were transferred from the stock cultures, and microbial suspensions were prepared in a nutrient broth for 24 hrs at 37°C until the turbidity of bacterial suspensions was achieved to 1.5×10^8 CFU mL^{-1} by comparison with the 0.5 McFarland standard. The assay was carried out by swabbing each test strain on the Mueller-Hinton agar plate using the 1/10 dilution of the microbial suspension. Sterile paper discs (Whatman No.1 filter paper) impregnated with 0.5 mg/mL and 1 mg/mL samples in DMSO were placed onto the surface of the agar plate at equal distances from each other. Chloramphenicol was used as a positive control. After overnight incubation at 37°C, zones of inhibition were measured. The samples were analyzed in triplicates.

2.6. *In-silico* Molecular Docking Analysis of the Isolated Compounds

The structures of the isolated compounds were drawn using ChemDraw 16.0. The molecules were treated quantum mechanically using the Gaussian 09 program suite at the Becke-3-Lee-YangPar (B3LYP) level combined with the standard 6-31G (d,p) basis set. All the parameters were set to get a stable structure with minimum energy. Each molecule's 3D coordinates (PDB) were obtained through the optimized structure. The crystal structures of *S. aureus* DNA Gyrase (PDB ID 2XCT) and human topoisomerase IIβ (PDB ID 3QX3) were downloaded from the protein data bank. The protein preparation was done using the reported standard protocol using AutoDock 4.2.6 (MGL tools 1.5.6). The AutoDock Vina searched for the best-docked conformation between isolated compounds and protein. A maximum of nine conformers were considered for each ligand in the docking process. The conformations with the least free binding energy were selected for analyzing the interactions between the target receptor and ligands by discovery studio visualizer and PyMOL. The molecular docking studies were carried out using AutoDock Tools (ADT) (Trott & Olson, 2010).

2.7. *In-silico* Pharmacokinetics and Toxicity of the Isolated Compounds

The structures of the isolated compounds were converted to their canonical simplified molecular-input line-entry system (SMILES) and submitted to the SwissADME tool to estimate *in-silico* pharmacokinetic parameters. The information about the number of hydrogen donors, hydrogen acceptors, rotatable bonds, and total polar surface area of the isolated compounds was obtained from the SwissADME predictor. The ligands were also subjected to Lipinski *et al*., screened using SwissADME and PreADMET predictors. The ligands' organ toxicities and toxicological endpoints and their LD_{50} were predicted using Pro Tox II and OSIRIS Property Explorer (Banerjee *et al*., 2018) (Garg, Tadesse, & Eswaramoorthy, 2021). The analyses of the compounds were compared with that of Doxycycline and Abiraterone standard drugs.

2.8. DFT Study

The isolated compounds were treated quantum mechanically with the DFT method using the Gaussian 09 program suite at the Becke-3-Lee-YangPar (B3LYP) level combined with the standard 6-31G (d,p) basis set without any symmetrical constraints. The DFT analysis of isolated compounds was performed using Gaussian 09 and visualized through Gauss view 6.0. The parameters were set to obtain a stable structure with minimum energy during the optimization procedure. The minimum global energy of the title compound was determined from the structure optimization procedure. The molecular electrostatic potential map and energies of the compounds were obtained from the optimized geometry. Koopman's approximation was used to estimate the HOMO-LUMO energy gap and related reactive parameters (electronegativity, chemical potential, hardness, softness, electrophilicity) (Abu-Melha, 2018; Vujovic *et al*., 2020).

3. RESULTS and DISCUSSION

3.1. Characterization

Seven compounds (Figure 1) were isolated and characterized in the present work. The structures of the compounds were established using various spectroscopic methods, including UV-Vis, IR, and NMR.

Figure 1. Chemical structures of isolated compounds.

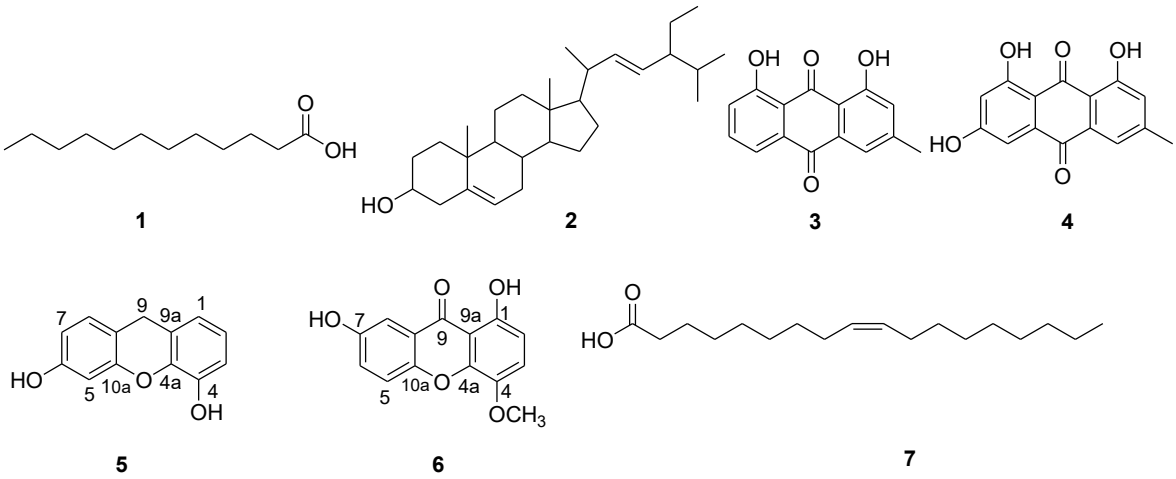

Compound **1**, obtained as a solid (19 mg), showed a spot on TLC at Rf. 0.75 with n-hexane: EtOAc (9:1) as a mobile phase. The IR and NMR spectral data of compound **1** agreed with the data reported for lauric acid (Yamashita *et al*., 2015).

Compound **2** (21 mg) was obtained as white crystals. The UV-Vis spectrum (ethanol) showed absorption maxima at 259 nm, indicating the presence of non-conjugated olefinic (C=C) groups. The IR (KBr) spectrum revealed the presence of O-H and C=C stretching at 3360 and 1638 cm^{-1}, respectively. The NMR spectral data of compound **2** were in good agreement with data reported for *β*-stigmasterol (Figure 1) (Chaturvedula & Prakash, 2012), which has been reported as a remedy for reducing the risk of heart disease and blood cholesterol. It also possesses potent laxative, antioxidant, antibacterial, hypoglycemic, and thyroid inhibiting properties (Panda *et al*., 2009).

Compound **3** (9 mg) was obtained as a yellow amorphous powder. The UV-Vis spectrum showed characteristic absorption bands for anthraquinone at λ_{max} 266, 288, and 435 nm (Coopoosamy & Magwa, 2006). The IR (KBr) spectrum displayed absorption band at 3433 cm^{-1} is due to O-H stretching. The NMR spectral data of **3** (Table 1) were compared with the literature reported for 1,8-dihydroxy-3-methylanthracene-9,10-dione (chrysophanol) and found in good agreement (Coopoosamy, & Magwa, 2006). So far, this compound has not been reported from the genus *Laggera*. Chrysophanol has been reported from *Aloe excelsa*, *Rheum emodi*, *Rhamnus prinoides*, *Rumex abyssinicus*, *Rumex japonicus*, and *Cassia tora* (Coopoosamy, & Magwa, 2006; Guo *et al*., 2011; Tamano & Koketsu, 1982).

Table 1. NMR spectral data of compound **3** and data reported for chrysophanol.

Carbon No	Compound 3		Lit. for chrysophanol
	^{1}H-NMR Data	^{13}C-NMR data	^{13}C-NMR data
1	–	162.4	162.4
2	7.12 (br. *s*, 1H)	124.5	124.5
3	–	149.3	149.3
4	7.67 (br. *s*, 1H)	119.9	119.9
5	7.83 (1H, *dd*, *J* = 1.2, 7.6 Hz)	136.9	136.9
6	7.69 (1H, *dd*, *J* = 8.4, 7.6 Hz)	124.4	124.4
7	7.30 (1H, *dd*, *J* = 1.2, 8.4 Hz)	121.4	121.4
8	–	162.7	162.7
9	–	192.5	192.5
10	–	182.0	181.9
11	–	133.6	133.6
12	–	115.9	115.7
13	–	113.7	113.4
14	–	133.3	133.3
15	2.48 (3H, s)	22.3	22.3

Chrysophanol has been reported as antimicrobial, anti-inflammatory, anti-mutagenic, and antidiabetic, inhibits poliovirus replication, and is active against HIV-1 protease (HIV-1 PR). The compound is also a potent photosensitizer (Rawat *et al*., 2013).

Compound **4** (13 mg) was obtained as an orange amorphous powder with an Rf. 0.55 in n-hexane:EtOAc (7:3) as a mobile phase. The UV-Vis spectrum (ethanol) displayed absorption bands at λ_{max} 250, 266, 289, and 436 nm characteristics of anthraquinone (Fekade, 2008). In the IR (KBr) spectrum, the absorption band at 3382 cm^{-1} is ascribed to O-H stretching. The NMR spectral analysis of compound **4** (Table 2) was in good agreement with the data reported for 1,6,8-trihydroxy-7-methylanthracene-9,10-dione, also known as emodin (Rawat *et al*., 2013) (Figure 1). Emodin has also not been reported from the genus but has been reported from *Senna occidentalis*, *Rheum palmatum*, *Rumex abyssinicus*, and the *Murrya koenigii*. The compound has been reported to possess antimicrobial, antiviral, anti-inflammatory, anti-ulcerogenic, immunosuppressive, and chemopreventive activities (Muto *et al*., 2007).

Table 2. NMR spectral data of compound **4** and data reported for emodin (Fekade, 2008).

Carbon No	Compound 4		Lit. for emodin
	^{1}H-NMR Data	^{13}C-NMR data	^{13}C-NMR data
1	–	162.3	162.4
2	7.12 (1H, m)	124.0	124.1
3	–	148.6	148.7
4	7.54 (1H, m)	120.5	120.6
5	7.23 (1H, *d*, *J* = 2.4 Hz)	108.8	108.8
6	–	165.5	165.5
7	6.65 (1H, *d*, *J* = 2.4 Hz)	107.9	107.9
8	–	165.3	165.4
9	–	190.7	190.9
10	–	181.2	181.3
11	–	135.6	135.4
12	–	109.5	109.6
13	–	113.5	113.6
14	–	133.3	133.4
15	2.46 (3H, s)	21.1	21.2

Compound **5** (17 mg) was obtained as a yellow crystal melting at 102°C. The IR spectrum showed an absorption band at 3394 cm^{-1} attributed to O-H stretching. The spectrum also displayed a band at 1610 cm^{-1} attributed to the C=C bond stretching of an aromatic ring. The ^{1}H NMR spectrum of compound **5** (Table 3) showed the presence of signals due to six protons on the aromatic ring. Three aromatic protons were observed at δ 7.54 (1H, d, J = 8.4 Hz), 6.89 (1H, d, J = 2.8 Hz), and 7.48 (1H, dd, J = 2.8, 8.4 Hz) were accounted to H-8, H-5, and H-7, respectively. The remaining at δ 7.26 (1H, dd, J = 2.8, 9.2 Hz), δ 7.41 (1H, dd, J = 7.2, 9.2 Hz), and δ 6.72 (1 H, d, J = 7.2 Hz) were due to the signals of H-3, H-2, and H-1, respectively. The spectrum also displayed a singlet signal at δ 3.48 (2H) diagnostic for the presence of methylene protons in the compound. The proton decoupled ^{13}C-NMR spectrum of compound **5** with the aid of DEPT-135 revealed the presence of 13 well-resolved carbon resonances, including one methylene, six methine, and six quaternary carbons. The signal due to methylene carbon is evident at δ 29.6. The remaining twelve signals were observed in the aromatic region, suggesting the presence of two non-equivalent aromatic rings in the structure of the compound. The signals in the aromatic ring were observed at δ 136.5 (C-8), 108.2 (C-7), 161.2 (C-6), 107.1 (C-5), 156.4 (C-10a), 128.1 (C-8a), 153.4 (C-4), 109.6 (C-3), 125.3 (C-2), 119.1 (C-1), 150.2 (C-4a) and at 128.6 (C-9a). Signals due to quaternary carbons were apparent at δ 161.2 (C-6), 156.4 (C-10a), 128.1 (C-8a), 153.4 (C-4), 150.2 (C-4a) and at 128.6 (C-9a). The most downfield signals at δ 161.2, 156.4, 153.4, and 150.2 are signals due to oxygenated aromatic carbons. The below spectral data led to the identification of compound **5** as 9H-xanthene-3, 5-diol, whose structure is depicted in Figure 1.

Table 3. ^{1}H NMR, ^{13}C NMR and DEPT-135 spectral data of compound **5**.

Position	^{1}H NMR δ (ppm)	^{13}C NMR δ (ppm)	DEPT-135
1	6.72 (1H, *d*, *J* = 7.2 Hz)	119.1	CH
2	7.41 (1H, *dd*, *J* = 7.2 and 9.2 Hz)	125.3	CH
3	7.26 (1H, dd, J = 2.8 and 9.2 Hz)	109.6	CH
4	–	153.4	Q
4a	–	150.2	Q
5	6.89 (1 H, *d*, *J* = 2.8 Hz)	107.1	CH
6	–	161.2	Q
7	7.48 (1H, *dd*, *J* = 2.8 and 8.4 Hz)	108.2	CH
8	7.54 (1 H, *d*, *J* = 8.4 Hz)	136.5	CH
8a	–	128.1	Q
9	3.48 (2H, s)	29.6	CH_2
9a	–	128.6	Q
10a	–	150.2	Q

Compound **6** (8 mg) was obtained as a yellow crystal, melting at 236-237°C. The IR spectrum revealed an absorption band at 3286 cm^{-1}, illustrating the presence of O-H stretching in the compound. The absorption band at 1667 cm^{-1} is presumably due to a conjugated carbonyl group. The absorption band due to the C=C bond is evident at 1640 cm^{-1}. The ^{1}H-NMR spectrum of compound **6** (Table 4) showed the presence of five protons on the aromatic ring. Two proton ortho coupled signals with AB multiplicity pattern at δ 6.61 (1H, d, J = 8.8 Hz) and at δ 7.17 (1H, d, J = 8.8 Hz) are accounted for the C-H aromatic protons on C-2 and C-3, respectively. Three aromatic protons were observed at δ 7.24 (1H, dd, J = 2.8 and 9.2 Hz), δ 7.42 (1 H, d, J = 9.2 Hz), and δ 7.45 (1 H, d, J = 2.8 Hz) for H-6, H-5, and H-8, respectively. The ^{1}H-NMR spectrum also displayed a signal from the methoxy group at δ 3.88. The ^{13}C-NMR spectrum of compound **6** in combination with DEPT-135 suggested the presence of 12

aromatic carbons, one methoxy carbon, and one C=O carbonyl carbon. The carbon signals resonating at δ 154.0 (C-1), 107.9 (C-2) 119.8 (C-3), 140.2 (C-4), 145.9 (C-4a) and 108.9 (C-9a) suggests the presence of six aromatic carbons. The spectrum also displayed other carbon resonances in the aromatic region at δ 119.3 (C-5), 125.3 (C-6), 153.8 (C-7), 108.1 (C-8), 120.0 (C-8a) and 150.1 (C-9a). The aromatic signals that bear hydroxyl groups were apparent at δ 153.8 and 154.0. The signals at δ 145.9 and 150.1 are accounted for the two quaternary carbons that bonded to the oxygen atom, hence assigned to C-10a and C-4a, respectively. The OH group must be situated para to the methoxy group to fit with that chemical shift (140.2 ppm), as reported in Yan (2001). The most downfield signal at δ 182.2 is characteristic of conjugated carbonyl (C-9). The signals which were not detected in the DEPT-135 NMR spectrum of compound **6**, including δ 108.9, 120.0, 140.2, 145.9, 150.1, 153.8, 154.0, and 182.2, were due to quaternary carbons. The signal due to the methoxy group was detected at δ 57.2.

Table 4. ^{1}H NMR, ^{13}C NMR, and DEPT-135 spectral data of compound **6**.

Position	^{1}H NMR δ (ppm)	^{13}C NMR δ (ppm)	DEPT 135 NMR
1	_	154.0	Q
2	6.61 (*1H, d, J* = 8.8 Hz)	107.9	(CH)
3	7.17 (1 *H, d J* = 8.8 Hz)	119.8	(CH)
4	_	140.2	Q
4a	_	145.9	Q
5	7.42 (1H, *d*, *J* = 9.2 Hz)	119.1	(CH)
6	7.24 (1H, *dd*, *J* = 2.8 and 9.2 Hz)	125.3	(CH)
7	_	153.8	Q
8	7.46 (1H, *d*, *J* = 2.8 Hz)	108.1	(CH)
8a	_	120.0	Q
9	_	182.2	Q
9a	_	108.9	Q
10a	_	150.1	Q
−OCH_3	3.88 (3H, s)	57.2	(CH_3)

With the above spectral data, compound **6** is identified as 1,7-dihydroxy-4-methoxyxanthone (Figure 1). Compound **7** was obtained as a white powder. The NMR spectral data and melting point of compound **7** is identical to oleic acid (Baker *et al*., 1995).

3.2. GC-MS analysis of the *n*-hexane extract of the roots of *L. tomentosa*

The essential oil of the roots of *L. tomentosa* has led to the identification of eleven major chemical constituents. It was found that the major component of the n-hexane extract of the root of *L. tomentosa* was 2,5-dimethoxy-*p*-cymene which constituted 59.39% followed by 1-isopropyl-2-methoxy-4-methylbenzene (9.54%), 2-(methylamino)-1-phenylethanol (7.56%), tetradecyl 2-(N-methylisobutyramido)acetate (6.54%), methyl palmitate (5.74%), 1-guanidinosuccinimide (3.77%), propanamide (1.96%), α-humulene (1.86%), N-methylpent-4-en-1-amine (1.29%), 2-fluoroamphetamine (1.20%) and sec-butylamine (1.15%). 2,5-Dimethoxy-*p*-cymene was also reported as one of the constituents from the essential oil of the aerial parts of *L. tomentosa* grown only in Ethiopia, which agrees well with the present work. However, the content of 2,5-dimethoxy-*p*-cymene reported from *L. alata* (44.2%) grown in Nigeria and *L. pterodonta* (30.5%) grown in the Benin Republic are inferior to the percent reported in this work (Omoregie, Okwute, & Koma, 2014; Verma *et al*., 2011; Hakim *et al*.,

2008). This compound was also reported from various plants' essential oils obtained from the family Asteraceae (Owolabi, Lajide, Villanueva, & Setzer, 2010). The presence of volatile components like 2,5-dimethoxy-*p*-cymene and 1-isopropyl-2-methoxy-4-methylbenzene suggests that the oil may be useful in aromatherapy, pharmaceuticals, and confectionery industries as fragrance or additives (Martin *et al*., 2000). The essential oils which contain this compound as a major component were reported to have antifungal (Hakim *et al*., 2008), antibacterial (Joshi, 2013), and insecticidal (Owolabi *et al*., 2010) properties. Therefore, the presence of 2,5-dimethoxy-*p*-cymene as a major constituent in the roots of *L. tomentosa* is one positive attribute of this plant.

3.3. Antioxidant Activities

3.3.1. *DPPH radical scavenging activity*

DPPH radical scavenging assay is a simple method for finding antioxidants by recording the absorbance at 517 nm (Brand-Williams, Cuvelier, & Berset, 1995). The extracts and isolated compounds from the roots of *L. tomentosa* were evaluated for their radical scavenging activities, and the result is presented in Table 5.

Table 5. DPPH Radical Scavenging Activities of the Extracts and Isolated Compounds (100 µg/mL).

Roots of *L. tomentosa*			Stem barks of *S. longipedunculata*		
Samples	% Inhibition	IC_{50} value	Samples	% Inhibition	IC_{50} value
n-hexane extract	55.8±0.3	92.0	*n*-hexane extract	42.0±0.8	218.0
EtOAc extract	84.3±0.2	9.4	EtOAc extract	89.1±0.7	7.4
MeOH extract	72.5±0.6	29.0	MeOH extract	91.0±0.3	6.4
2	37.8±0.4	1150.0	**5**	88.0±0.6	8.4
3	86.0±0.6	6.2	**6**	90.2±0.5	4.2
4	92.0±0.1	3.8	**Ascorbic acid**	97.0±009	3.38

Samples were reported as Mean ± SEM; IC_{50} values were reported in µg/mL

As shown in Table 5, the *n*-hexane extract of the roots of *L. tomentosa* inhibited the DPPH radical by 55.8%. The percentage inhibitions of the EtOAc and MeOH extracts and compounds **2**, **3**, and **4** are 84.3, 72.5, 37.8, 86.0, and 92%, respectively. The IC_{50} values were 92, 9.4, 29, 1150, 6.2, and 3.8 µg/mL for hexane, EtOAc, and MeOH extract, and compounds **2**, **3**, and **4** isolated from the roots of *L. tomentosa*, respectively. The corresponding result of 3.38 µg/mL was recorded for ascorbic acid. As clearly revealed from Table 1, compounds **3**, **4**, and the EtOAc extract displayed comparable radical scavenging activities with the standard. This activity is likely due to hydroxyl groups in anthraquinones **3** and **4**. The behavior agrees with the IC_{50} values of compounds **3** (6.2 µg/mL) and **4** (3.8 µg/mL). Therefore, the results showed that the roots of *L. tomentosa* can serve as a source of radical scavenging compounds and hence can be utilized as a natural antioxidant.

The hexane, EtOAc, and MeOH extract of the stem barks of *S. longipedunculata* inhibited DPPH radical by 42, 89, and 91% (Table 5). This percentage indicates that the MeOH and EtOAc extract inhibited the DPPH radicals significantly compared with the hexane extract. This activity might be due to flavonoids and was confirmed using Salkowski Test in the EtOAc and MeOH extracts compared to the *n*-hexane extract. This result is also evident from the low IC_{50} of the EtOAc (7.42 µg/mL) and MeOH extract (6.48 µg/mL). At the same concentration, ascorbic acid scavenged the DPPH radical by 97.0% with an IC_{50} value of 3.38. Compounds **5** and **6** inhibited DPPH radical by 88 and 90.2%, respectively. The result is almost close to ascorbic acid used as a positive control. Therefore, the observed high free radical scavenging

activity of the EtOAc and MeOH extract may be accounted to the presence of compounds **5** and **6**, isolated in this study from the stem bark of *S. longipedunculata*.

3.3.2. *Ferric thiocyanate method*

The degree of lipid peroxidation, which was evaluated using the ferric thiocyanate method, can measure the antioxidant potential of compounds or extracts. Table 6 is the result of the anti-lipid peroxide formation of the constituents of *L. tomentosa* and *S. longipedunculata*.

Table 6. Anti-lipid peroxidation activities of constituents of *L. tomentosa* and *S. longipedunculata.*

Stem bark of *S. longipedunculata*		Roots of *L. tomentosa*	
Samples	% Inhibition	Samples	% Inhibition
n-hexane extract	47.2±0.4	*n*-hexane extract	35.2±0.2
EtOAc extract	70.8±1.0	EtOAc extract	78.5±0.8
MeOH extract	76.4±0.7	MeOH extract	74.1±1.1
5	79.2±0.1	Ascorbic acid	84.7±0.4
6	81.9±0.3		

Samples were reported as Mean ± SEM; Ascorbic acid was used as positive control

As depicted in Table 6, the anti-lipid peroxidation activity of the *n*-hexane extract is inferior to the other extracts and isolated compounds. On the other hand, the EtOAc and MeOH extracts of *S. longipedunculata* inhibited peroxide formation by 70.8 and 76.4%, respectively, demonstrating their potential in preventing the formation of lipid peroxides. The results turned out to be comparable with ascorbic acid, which inhibits the formation of lipid peroxides by 84.7%. Likewise, compounds **5** and **6** were shown to have a high ability to inhibit peroxide formation, which is comparable with ascorbic acid. The anti-lipid peroxidation activity of the *n*-hexane, EtOAc, and MeOH extracts of the roots of *L. tomentosa* displayed % inhibition of 35.2, 78.5, and 74.1%, respectively. The result demonstrated by EtOAc extract is close to ascorbic acid.

3.4. Antibacterial Activity

The extracts and isolated compounds from *L. tomentosa* were assayed *in-vitro* against *S. aureus*, *E. coli*, *P. mirabilis*, and *K. pneumoniae* (Table 7). The MeOH and *n*-hexane extracts were significantly active against *S. aureus* and *E. coli* at 1.0 mg/mL, displaying an inhibition zone of 11-13 mm. The EtOAc extract had an IZ of 12 mm against *E. coli* than other strains used in this study. At 0.5 mg/mL, EtOAc and MeOH extracts demonstrated moderate antibacterial effects (7-10 mm) against all the tested bacteria, indicating that the samples inhibit the pathogens in a dose-dependent manner. The activity of EtOAc and MeOH extract (at 1 mg/mL concentration) of the roots of *L. tomentosa* against the Gram-negative [*K. pneumoniae* (10 mm, 9 mm), *E. coli* (12 mm, 12 mm), and *P. mirabilis* (11 mm, 9 mm)] respectively is impressive because Gram-negative bacteria tend to have higher intrinsic resistance to most antimicrobial agents (Ndukwe, Okeke, Lamikanra, Adesina, & Aboderin, 2005). Compounds **1**, **2**, and **3** isolated from this plant were shown to have a high zone of inhibition with diameters of (10 mm, 8 mm, and 11 mm), (12 mm, 11 mm, and 10 mm), and (13 mm, 11 mm and 9 mm) against *S. aureus*, *K. pneumoniae*, and *E. coli*, respectively. However, the activity displayed by these compounds is inferior to compound **4**. Hence, fractionations of the active EtOAc extract of *L. tomentosa* over silica gel column chromatography traced the activity to emodin (4) with an inhibition zone of 18 mm against *S. aureus*. This agreement is consistent with the solid antimicrobial activities reported for compound **4** from different sources (Muto *et al*., 2007). Hence, the result obtained in the present study supports the traditional use of *L. tomentosa* against diseases caused by bacteria.

Table 7. Zone of Bacterial Growth Inhibition (mm) of Extracts and Isolated Compounds.

Samples	Roots of *L. tomentosa*				
	Conc. in mg/mL	Zones of inhibition in mm			
		S. aureus	*K. pneumoniae*	*E. coli*	*P. mirabilis*
n-hexane extract	0.5	NI	7.10±0.40	NI	NI
	1.0	12.00±0.20	10.21±0.30	11.01±0.10	NI
EtOAc extract	0.5	9.01±0.41	7.10±0.21	10.01±0.30	8.10±0.40
	1.0	19.01±0.31	10.00±0.30	12.10±0.20	11.10±0.40
MeOH extract	0.5	8.10±0.30	9.01±0.20	9.20±0.21	8.10±0.20
	1.0	13.00±0.20	7.00±0.21	12.20±0.40	9.10±0.20
1	0.5	8.20±0.30	7.10±0.20	8.10±0.30	NI
	1.0	10.21±0.20	8.21±0.20	11.20±0.21	NI
2	0.5	8.40±0.30	10.00±0.40	9.00±0.20	8.11±0.30
	1.0	12.00±0.20	11.10±0.41	10.10±0.30	10.11±0.11
3	0.5	7.10±0.10	8.10±0.10	7.10±0.10	NI
	1.0	13.00±0.20	11.21±0.30	9.10±0.10	NI
4	0.5	8.00±0.20	10.21±0.10	7.20±0.21	NI
	1.0	18.00±0.10	12.10±0.30	8.20±0.20	NI
Chloramphenicol	1.0	18.00±0.10	18.10±0.10	18.20±0.10	18.10±0.11
Stem barks of S. longipedunculata					
Samples	Conc. in mg/mL	Zones of inhibition in mm			
		E. coli	*S. aureus*	*S. typhi*	*B. subtilis*
n-hexane extract	0.5	8.10±0.22	10.04±0.23	6.01±0.21	NI
	1.0	12.10±0.02	14.04±0.07	7.08±0.31	NI
EtOAc extract	0.5	7.00.09±0.02	11.00±012	9.09±0.21	NI
	1.0	11.08±0.04	15.03±018	12.09±0.42	NI
MeOH extract	0.5	7.11±0.03	9.00±0.33	7.20±0.21	NI
	1.0	11.21±0.07	12.00±0.28	8.00±0.31	NI
5	0.5	8.11±0.10	12.00±0.09	10.10±0.21	NI
	1.0	11.31±0.10	15.09±0.09	15.12±0.31	6.00±0.03
6	0.5	9.21±0.21	11.26±0.11	12.11±0.07	6.40±0.11
	1.0	14.19±0.14	16.06±0.22	15.28±0.09	8.20±0.21
Chloramphenicol	1.0	18.20±0.10	18.10±0.10	19.20±0.30	21.10±0.19

NI: no inhibition; Results are mean ± SD of triplicate experiments

Likewise, the extracts and isolated compounds from *S. longipedunculata* were assessed for their *in-vitro* antibacterial activity against *E. coli*, *S. aureus*, *S. typhi*, and *B. subtilis*. The results are summarized in Table 7. The *n*-hexane, EtOAc, and MeOH extracts of *S. longipedunculata* showed inhibition zones of 14.04±0.07, 15.03±018, and 12.00±0.28 against *S. aureus* at 1 mg/mL. On the other hand, the EtOAc extract of *S. longipedunculata* showed an inhibition zone of 12.09±0.42 against *S. typhi*, while the *n*-hexane and MeOH extract were turned out to be inactive. This result was in close agreement with the one reported in the literature on the same bacterial strain (Declercq *et al*., 2001). None of the extracts and isolated compounds demonstrated activity against *B. subtilis*. Fractionation of the active EtOAc extract has led to the isolation of two xanthones that displayed activity against *S. aureus*, *E. coli*, and *S. typhi*. Compound **5** exhibited inhibition zones of about 11.31±0.10, 15.09±0.09, and 8.00±0.31

against *E. coli*, *S. aureus*, and *S. typhi*, respectively. Likewise, compound **6** displayed an inhibition zone of 14.19±0.14, 16.06±0.22, and 15.28±0.09, respectively. As clearly observed from Table 3, compounds **5** and **6** displayed similar activity with the standard drug against *S. aureus* with an inhibition zone of 15.09±0.09 and 16.06±0.22 mm, respectively. Therefore, the activity shown by the extract could be accounted to the presence of the two xanthones in the extract.

3.5. Molecular Docking Studies

Molecular docking studies are generally employed to investigate the binding energy and to further validate the molecular mechanisms for ligands at the active site of a protein. All the isolated compounds were subjected to molecular docking studied against selected proteins viz. *S. aureus* DNA Gyrase (PDB ID 2XCT) and human topoisomerase IIβ with DNA (PDB ID 3QX3) using Auto-dock Vina (Trott & Olson, 2010) to find out the binding mode.

S. aureus DNA Gyrase, an enzyme belonging to a member of bacterial topoisomerase, controls the topology of DNA during transcription, replication, and recombination by introducing short breaks to both DNA strands. Hence, the bacterial gyrase is paramount for bacterial survival and, therefore, necessary to disrupt as an antibacterial drug target (El-Etrawy & Sherbiny, 2021). Therefore, in this study, the molecular docking analysis of the isolated compounds was carried out to investigate their binding pattern with bacterial gyrase. The results were compared with standard antibacterial agents ciprofloxacin and doxycycline. The isolated compounds were found to have minimum binding energy ranging from – 4.8 to – 10.4 kcal/mol (Table 8). Compounds **1** (Arg-458), **2** (Glu-1088), **3** (Asp-437, Gly-459), and **4** (Gly-459) have shown hydrogen bonding interaction with various amino acid residues, and few additional hydrogen-bonding interactions are also shown with bacterial DNA (Table 8). Compounds **5-6** showed the residual amino acids interactions with Ala-47, Glu-50, Gly-77, Ile-78, Pro-79, Ile-94, Thr-165 (Hydrophobic), and Asp-73, Arg-76, Asn-46 (Hydrogen bond) similar to ciprofloxacin and doxycycline within the binding site of the protein. Compound 5 forms hydrogen bond interaction with Arg-76, Gly-77, and Thr-165 in the target protein's active site with lower binding affinity − 6.7 kcal/mol. The lowest binding score was displayed by compound **1** (–4.8 kcal/mol), while the best result was achieved using compounds **3** and **4** (–10.4 kcal/mol), with their affinity, found to be comparable to doxycycline (– 13.0 kcal/mol) and ciprofloxacin (– 8.4 kcal/mol) (Figure 2). The *in-silico* molecular docking analysis was also found to agree with *in-vitro* results. Hence, these compounds might have the potential to be promising antibacterial agents. The binding affinity, H-bond, and residual interaction of all the isolated compounds are summarized in Table 8.

Table 8. Molecular docking results of isolated compounds against *S. aureus* DNA Gyrase.

Ligands	Binding affinity (kcal/mol)	H-bond	Residual interactions	
			Hydrophobic and Electrostatic	Van der Waals
1	−4.8	Arg-458: HH11, Arg-458: CD, DC-12, DG-9	Hydrophobic-Pi-Sigma-DG-9; Hydrophobic-Pi-Sigma-DT-8; Hydrophobic-Alkyl-Arg-458; Hydrophobic-Pi-Alkyl-DG-9(Dist. 5.11974 Å); Hydrophobic-Pi-Alkyl-DG-9(Dist. 4.51935 Å) and Hydrophobic-Pi-Alkyl-DA-13	Asp-437, DT-10
2	−8.2	Glu-1088	Hydrophobic-Alkyl-Ala-1120(Dist. 4.63949 Å); Hydrophobic-Alkyl-Ala-1120(Dist. 4.22537 Å); Hydrophobic-Pi-Alkyl-DG-9(Dist. 5.37583 Å)	Arg-1122, Asp-1083, Met-1121, Ala-1119, Ser-1084,
3	−10.4	Asp-437, Gly-459	Hydrophobic-Pi-Sigma-Arg-DT-8;Hydrophobic-Pi-Sigma-DG-9(Dist. 3.44611 Å); Hydrophobic-Pi-Pi Stacked-DA-13; Hydrophobic-Pi-Alkyl-DT-8	Leu-457, Arg-458, Phe-1123, Arg-1122, Gly-436
4	−10.4	Gly-459, DG-9, DA-13, UNK0:H	Hydrophobic-Pi-Pi Stacked-DT-8(Dist. 3.96173 Å); Hydrophobic-Pi-Pi Stacked-DT-8(Dist. 5.03189 Å); Hydrophobic-Alkyl-Arg-458	DC-12
5	−6.7	Arg-76, Gly-77, Thr-165	Asn-46, Glu-50, Ile-78, Val-167	Asp-73, Ala-47, Gly-75, Val
6	−9.9	Gly-77, Glu-50	Asn-46, Arg-76, Ile-78, Pro-79	Asp-73, Ala-47, Thr-165
Doxycycline	−13.0	Ser-438, Ser-1084, Arg-1122	Electrostatic-Attractive Charge-Asp-1083; Hydrophobic-Pi-Alkyl-Ala-1120(Dist. 4.02007 Å); Hydrophobic-Pi-Alkyl-Ala-1120(Dist. 4.00436 Å)	Arg-1122, Met-1121, Phe-1123, Asp-437, DG-9
Ciprofloxacin	−8.4	Arg-1122, Asp-1083, Ala-1118, DG-9	Hydrophobic-Pi-Pi-T-Shaped-DG-9;Hydrophobic-Pi-Alkyl-DG-9;Hydrophobic-Pi-Alkyl-Ala-1120	DA-11, DT-10, Gly-1082, Phe-1123, Ser-438, Asp-437

The 2D and 3D binding interactions of compound **4** against *S. aureus* DNA Gyrase are depicted in Figure 2. 3D Ribbon and line models show the binding pocket structure of *S. aureus* DNA Gyrase with compound **4**. Hydrogen bonds between compounds and amino acids are shown as green dash lines, hydrophobic interactions are shown as pink/purple lines.

Figure 2. The 2D and 3D binding interactions of compound **4** against *S. aureus* DNA Gyrase.

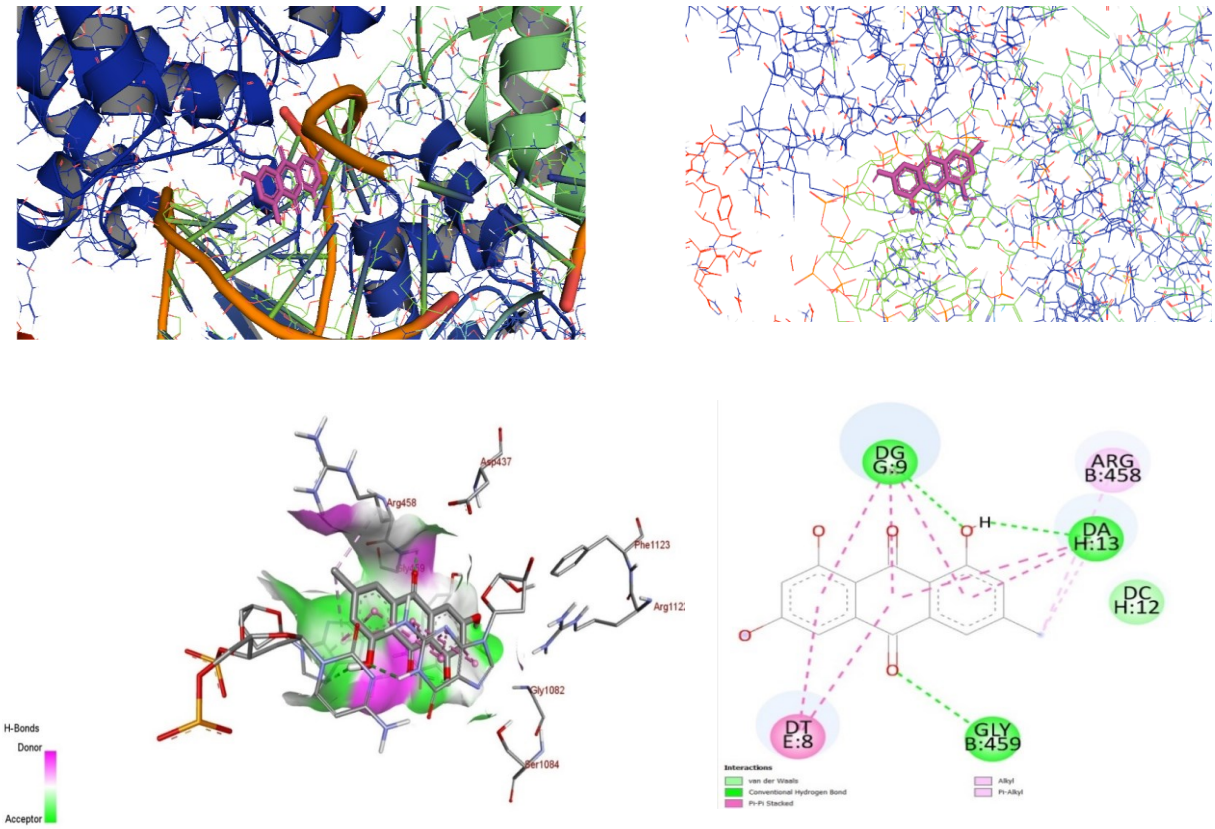

3.6. Binding mode of isolated compounds docked against human topoisomerase IIβ

In this study, the molecular docking analysis of the isolated compounds was carried out to investigate their binding interaction within the binding sites of human topoisomerase IIβ and the results were compared with standard anti-cancer agents vosaroxin and abiraterone. The isolated compounds were found to have minimum binding energy ranging from – 5.6 to – 10.4 kcal/mol (Table 9). Compared with vosaroxin (– 10.2 kcal/mol) and abiraterone (– 11.8 kcal/mol), the isolated compounds have shown comparable binding affinity and residual and DNA interaction profiles with various amino acid residues. The *in-silico* interaction results have shown that the isolated compounds have a comparable binding affinity with abiraterone; among them, compounds **3** (– 9.8 kcal/mol) and **4** (– 10.4 kcal/mol) revealed good binding affinity (Figure 3). Compound **1** has shown lower docking affinity (–5.6 kcal/mol) but good matching amino acid residues interactions compared to vosaroxin and abiraterone. Based on the molecular docking analysis results, the isolated compounds have shown comparable residual interactions and docking scores with vosaroxin and abiraterone. Hence, compounds **3** and **4** might prove to be good anti-cancer agents. The binding affinity, H-bond, and residual interaction of all the isolated compounds are summarized in Table 9. However, *in-vitro* analysis has not been performed for anti-cancer activity, but promising *in-silico* results reflect that further analysis might be fruitful.

Table 9. Molecular docking results of isolated compounds against human topoisomerase IIβ.

Compounds	Binding Affinity (kcal/mol)	H-bond	Residual interactions	
			Hydrophobic	Van der Waals
1	− 5.6	Lys-456: HZ1, Lys-456: HZ3, DT-9	Hydrophobic-Alkyl-Arg-503 (Dist. 4.12106 Å); Hydrophobic-Alkyl-Arg-503 (Dist. 4.91145 Å); Hydrophobic-Pi-Alkyl-DC-8	Asp-479, Gly-478, Gly-504, DA-12
2	− 9.1	Asn-786, DG-5	Hydrophobic-Alkyl-Met-782(Dist. 4.0209 Å); Hydrophobic-Alkyl-Met-782(Dist. 4.73849 Å); Hydrophobic-Alkyl-Val-785(Dist. 4.37004 Å); Hydrophobic-Alkyl-Val-785(Dist. 5.11179 Å); Hydrophobic-Alkyl-Ala-816(Dist. 5.08237 Å); Hydrophobic-Alkyl-Ala-816(Dist. 4.35645 Å); Hydrophobic-Alkyl-Pro-819	Ser-818, Arg-820, Gln-778, Lys-814, Gly-813, Gln-789, Gly-812, DG-10, DC-11, DT-9, DA-12
3	− 9.8	Asp-479: HN, Asp-479: OD1, Arg-503, DT-9, DG-10, UNK0:H	Hydrophobic-Pi-Sigma-Arg-503(Dist. 3.835 Å); Hydrophobic-Pi-Sigma-Arg-503(Dist. 3.88167 Å); Hydrophobic-Pi-Pi T-Shaped-DG-13; Hydrophobic-Pi-Alkyl-Arg-503	Ser-480, Gly-478, Gly-504, Glu-477, DA-12, DC-8
4	− 10.4	Asp-479, DT-9, DG-10, UNK0:H	; Hydrophobic-Pi-Sigma-Arg-503; Hydrophobic-Pi-Pi T-Shaped-DG-13(Dist. 5.81293 Å); Hydrophobic-Pi-Pi T-Shaped-DG-13(Dist. 5.18989 Å); Hydrophobic-Pi-Alkyl-Arg-503	Gly-504, Glu-477, Gly-478, Ser-480, Lys-456, DC-8, DA-12,
Abiraterone	-11.8	DG-10	Hydrophobic-Alkyl-Arg-503(Dist. 4.50057 Å); Hydrophobic-Alkyl-Arg-503(Dist. 4.19301 Å); Hydrophobic-Pi-Alkyl-DA-12; Hydrophobic-Pi-Alkyl-DC-8	Gly-504, Glu-477, Gly-478, Lys-456, Asp-479, DT-9
Vosaroxin	− 10.2	Gln-778, DC-8, DG-10, DG-13	Pi-Sulfur-DT-9; Hydrophobib-Pi-Pi-Stacked-DT-9 (Dist. 5.68139 Å); Hydrophobib-Pi-Pi-Stacked-DT-9 (Dist. 4.27157 Å); Hydrophobic-Pi-Alkyl-Arg-503	Gly-776, DA-12, Lys-456

The 2D and 3D binding interactions of compound **4** against human topoisomerase IIβ (PDB ID 3QX3) are presented in Figure 3. 3D Ribbon and line models show the binding pocket structure of human topoisomerase IIβ with compound **4**. Hydrogen bonds between compounds and amino acids are shown as green dash lines, hydrophobic interactions are shown as pink lines.

Figure 3. The 2D and 3D binding interactions of compound **4** against human topoisomerase IIβ (PDB ID: 3QX3).

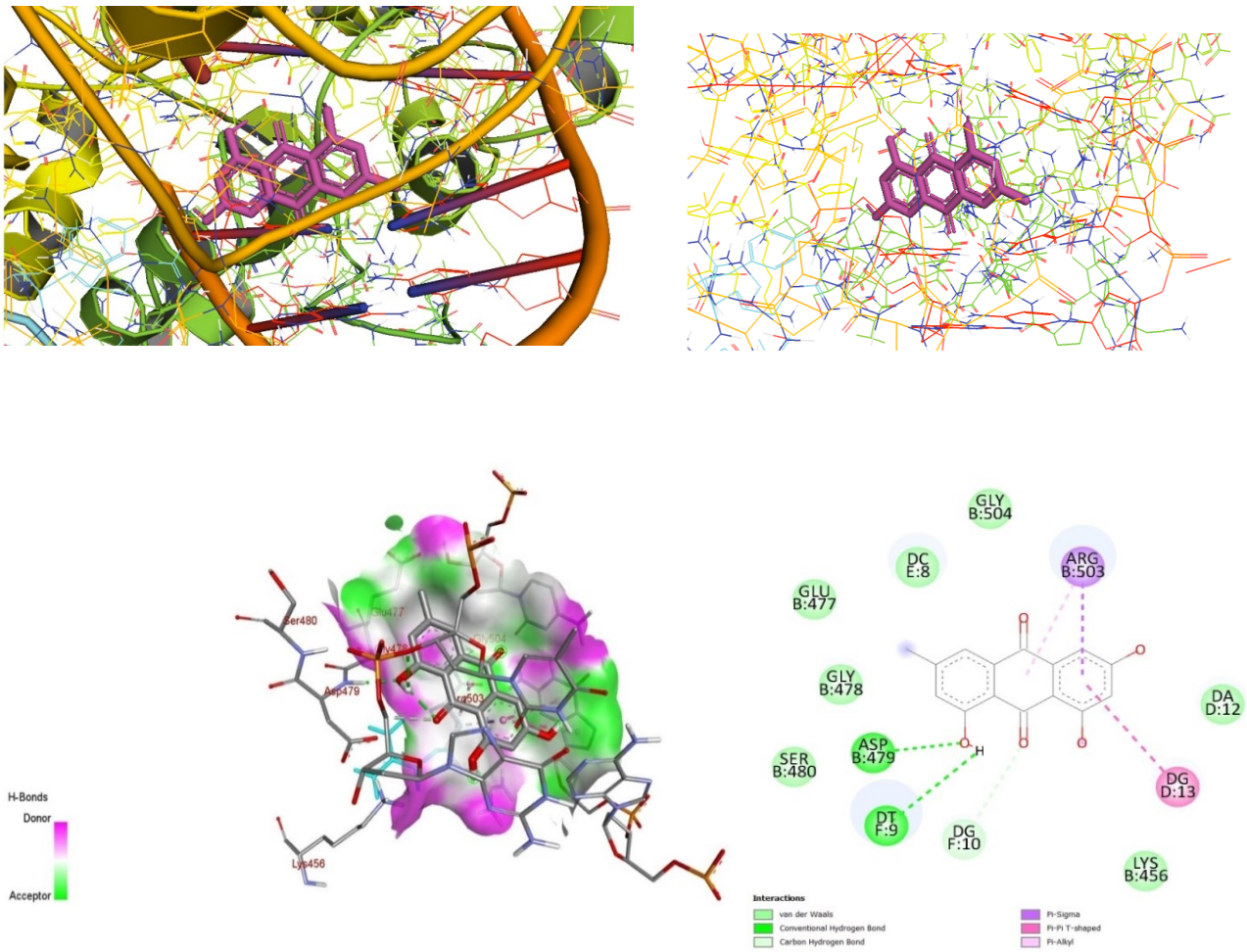

3.7. *In-silico* Pharmacokinetics (Drug-likeness) and Toxicity analysis

Drug-likeness is a prediction that determines whether a particular pharmacological agent has properties consistent with being an orally active drug. Lipinski's rule described that potential drug-like molecules should have the following properties: (i) less than five hydrogen-bond donors (HBDs), (ii) less than ten hydrogen-bond acceptors (HBAs), (iii) a molecular mass less than 500 Da, and (iv) log P not more than five and (v) total polar surface area (TPSA) should not be > 140 Å (Lipinski, Lombardo, Dominy, & Feeney, 2001). The results obtained in the present work revealed that all compounds satisfy Lipinski's rule of five (Table 10) (Ah & Yi, 2019). Hence, all the isolated compounds might be candidates for anti-cancer, antioxidant, and antimicrobial studies. Acute toxicity predictions result such as LD_{50} values, and toxicity class classification [1 (toxic) to 6 (non-toxic)] reveal that none of the ligands has shown acute toxicity and were found to be similar to standard drugs. The isolated compounds **1** and **2** have shown toxicity class classification 4 (harmful if swallowed), while **3** and **4** showed even better toxicity class 5. The toxicological prediction gives results of endpoints such as Hepatotoxicity, Carcinogenicity, mutagenicity, immunogenicity, and cytotoxicity. All the isolated compounds were predicted to be non-hepatotoxic, non-carcinogenic, non-irritant, and non-cytotoxic.

However, compounds **2** and **3** have shown immunotoxicity, while **3** and **4** have mutagenicity. Hence, based on ADMET prediction analysis, none of the compounds have shown acute toxicity, so that they might be proven as good drug candidates.

Table 10. Drug-likeness predictions of compounds, computed by SwissADME.

Ligands	Formula	Mol. Wt. (g/mol)	NRB	NHA	NHD	TPSA ($A^{°2}$)	Log *P* (iLOGP)	Log *S* (ESOL)	Lipinski's rule of five
1	$C_{12}H_{24}O_2$	200.32	10	2	1	37.30	2.70	-3.07	0
2	$C_{29}H_{50}O$	414.71	5	1	1	20.23	5.01	-7.99	1
3	$C_{15}H_{10}O_4$	254.24	0	4	2	74.60	2.22	-4.11	0
4	$C_{15}H_{10}O_5$	270.24	0	5	3	94.83	1.80	-3.67	0
5	$C_{13}H_{10}O_3$	214.22	0	3	2	49.69	2	-3.45	0
6	$C_{14}H_{10}O_5$	258.23	1	5	2	79.9	2.29	-3.37	0
Abirater-one	$C_{24}H_{31}NO$	349.51	1	2	1	33.12	3.42	-5.03	1
Doxycy-cline	$C_{22}H_{24}N_2O_8$	444.43	2	9	6	181.62	1.11	-2.59	1

NHD: number of hydrogen donors; NHA: number of hydrogen acceptors; NRB: number of rotatable bonds; TPSA: total polar surface area.

3.8. DFT Study

The structures of the isolated compounds, along with force on the nucleus, were optimized to find out the minimum global energy by the DFT. The energy difference between the Highest Occupied Molecular Orbital (HOMO) and the Lowest Unoccupied Molecular Orbital (LUMO) is an excellent indicator of electronic transition absorption in molecular systems. These provide insight into the reactivity of molecules. Owing to the HOMO–LUMO orbital interaction, LP-LP, and LP-bond pair type interactions were predominant in the investigated compounds. The calculated HOMO, LUMO energies, the energy gap, and dipole moment are shown in Table 11. The molecular orbital analysis for the investigated compounds based on their optimized geometry indicates that the frontier molecular orbitals are mainly composed of p-type atomic orbitals. An electronic system with a more significant HOMO-LUMO gap is less reactive than one with a smaller gap. Moreover, the HOMO–LUMO energy gap clearly explains the eventual charge transfer within the molecule. The power of an electronegative atom in a compound to attract an electron towards it was introduced by Pauling. The parameters such as hardness (η), ionization potential (I), electronegativity (χ), chemical potential (μ), electron affinity (A), global softness (σ), and global electrophilicity (ω) are calculated.

The ionization energy (IE) can be expressed through HOMO orbital energies, and electron affinity (EA) can be expressed through LUMO orbital energies. The hardness (η) corresponds to the HOMO and LUMO orbital energies gap, and the hardness has been associated with the stability of the chemical system. All the calculated values of quantum chemical parameters of the investigated molecules using the B3LYP method with 6-31G (d,p) basis-set are summarized in Table 11. From the results in Table 11, it is clear that for the molecules investigated, **4** has the minimum energy gap of 3.36138 eV, and **1** has the maximum energy gap of 7.58948 eV. These facts further indicate that compound **4** would be highly reactive among all the isolated compounds. All calculated values indicate the extensive charge delocalization in the investigated molecules, and the positive charges are localized over the hydrogen atoms.

The electron density is key to the bonding and geometry because the forces holding the nuclei together in a molecule are the attractive forces between the electrons and the nuclei. These attractive forces are opposed by the repulsion between the electrons and the repulsion between the nuclei. In the equilibrium geometry of a molecule, these electrostatic forces just balance. The fundamentally important Hellman–Feynman theorem (Popelier, 2000) states that

the force on a nucleus in a molecule is the sum of the coulombic forces exerted by the other nuclei and by the electron density distribution ρ. This distribution means that the energy of interaction of the electrons with the nuclei can be found by considering the classical electrostatic forces between the nuclei and the electronic charge cloud. The atoms are held together by the electrostatic force exerted by the electronic charge on the nuclei. Nevertheless, quantum mechanics, particularly the Pauli principle, determines the distribution of electronic charges. All these compounds have shown balanced charge distribution, which makes them adhesive to various biological enzymes.

Table 11. The various Quantum chemical parameters of isolated compounds.

S. No	Optimized energy (Hartree)	E_{HOMO} (eV)	E_{LUMO} (eV)	Energy Gap ΔE (eV)	Electro-negativity χ (eV)	Pauling Hardness η (eV)	Global Softness σ (eV^{-1})	Global Electrophilicity ω (eV)	Dipole Moment (Debye)
1	-622.2564	-7.2913	0.2982	7.5895	3.4966	3.7947	0.26352	1.6109	1.8706
2	-1210.479	-6.3799	0.7187	7.0986	2.8306	3.5493	0.28175	1.1287	1.3978
3	-878.5809	-6.4028	-3.0275	3.3753	4.7151	1.6876	0.59254	6.5869	1.0981
4	-953.8046	-6.3405	-2.9792	3.3614	4.6598	1.6807	0.59499	6.4599	2.4802

4. CONCLUSION

In this work, seven compounds such as lauric acid (1), *β*-stigmasterol (2), chrysophanol (3), emodin (4), 9H-Xanthene-3,5-diol (5), 1,7-dihydroxy-4-methoxyxanthone (6) and oleic acid (7) were isolated. Compounds **3** and **4** are new to the genus Laggera, while compounds **5** and **6** are new to the species *S. longipedunculata*. GC-MS analysis of the essential oil of the roots of *L. tomentosa* gave 2,5-dimethoxy-*p*-cymene as the principal constituent (59.39%), suggesting the use of the root of *L. tomentosa* as antibacterial agents. The antioxidant activity of the EtOAc extract, emodin (4), and 1,7-dihydroxy-4-methoxyxanthone (6) was found to be close to ascorbic acid, indicating the strong ability of the extract of the plant as radical scavengers and inhibitors of lipid peroxidation. The extracts of *L. tomentosa* and *S. longipedunculata* showed better antibacterial activity in a dose-dependent manner against *S. aureus*, with activity traced to compounds **4** and **6**, respectively. These compounds also displayed comparable binding affinities to ciprofloxacin and doxycycline against *S. aureus* DNA Gyrase, proposing that compounds **4** and **6** might be used as lead compounds for further development as antibacterial agents. Compound **4** also displayed a comparable affinity with vosaroxin and abiraterone against human topoisomerase IIβ. Hence, emodin (4) might be considered a lead compound for further development as an anti-cancer agent. Furthermore, the presence of emodin and chrysophanol and their immense biological activities demonstrate the positive attributes of the root of *L. tomentosa*.

Acknowledgments

The authors are grateful to Adama Science and Technology University for funding.

Declaration of Conflicting Interests and Ethics

The authors declare no conflict of interest. This research study complies with research and publishing ethics. The scientific and legal responsibility for manuscripts published in IJSM belongs to the authors.

Authorship contribution statement

Yadessa Melaku, Tokuma Getahun, Markos Addisu and **Hailemichael Tesso** were responsible for the isolation, antibacterial, and antioxidant activities of the isolated compounds from *L. tomentosa* and *S. longipedunculata.* The *in-silico* molecular docking analysis and DFT

study were performed by **Rajalakshmanan Eswaramoorthy** and **Ankita Garg**. The write-up of the manuscript was done by all authors.

Orcid

Yadessa Melaku https://orcid.org/0000-0003-2599-0517
Tokuma Getahun https://orcid.org/0000-0003-4564-9252
Markos Addisu https://orcid.org/0000-0004-4150-8819
Hailemichael Tesso https://orcid.org/0000-0012-5423-7845
Rajalakshmanan Eswaramoorthy https://orcid.org/0000-0002-8331-2100x
Ankita Garg https://orcid.org/0000-0003-0200-1376

REFERENCES

Abu-Melha, S. (2018). Design, Synthesis and DFT/DNP Modeling Study of New 2-Amino-5-arylazothiazole Derivatives as Potential Antibacterial Agents. *Molecules, 23*(2). https://doi.org/10.3390/molecules23020434

Ah, A., & Yi, A. (2019). In silico Pharmacokinetics and Molecular Docking Studies of Lead Compounds Derived from Diospyros Mespiliformis. *PharmaTutor*, 7, 31-37.

Akpemi, A., Oyewale, A.O., Ndukwe, I.G. (2013). *Phytochemical screening and antimicrobial activity of extracts of Securidaca longepedunclata root bark MeOH extract*. [Department of Chemistry, Thesis, Federal Collage of Education, Zaria, Nigeria].

Asfaw, N., Storesund, H.J., Aasen, A.J., & Skattebol, L. (2003). Constituents of the Essential Oil of Laggera tomentosa Sch. Bip. ex Oliv. et Hiern Endemic to Ethiopia. *Journal of Essential Oil Research, 15*(2), 102-105. https://doi.org/10.1080/10412905.2003.9712081

Baker, J.T., Borris, R.P., Carté, B., Cordell, G.A., Soejarto, D.D., Cragg, G.M., . . . Tyler, V. E. (1995). Natural product drug discovery and development: new perspectives on international collaboration. *J Nat Prod, 58*(9), 1325-1357. https://doi.org/10.1021/np50123a003

Banerjee, P., Eckert, A.O., Schrey, A.K., & Preissner, R. (2018). ProTox-II: a webserver for the prediction of toxicity of chemicals. *Nucleic Acids Res, 46*(W1), W257-w263. https://doi.org/10.1093/nar/gky318

Brand-Williams, W., Cuvelier, M.E., & Berset, C. (1995). Use of a Free Radical Method to Evaluate Antioxidant Activity. *Lwt - Food Science and Technology, 28*, 25-30.

Chaturvedula, V., & Prakash, I. (2012). Isolation of Stigmasterol and ?-Sitosterol from the dichloromethane extract of Rubus suavissimus. *International Current Pharmaceutical Journal, 1*(9), 239-242. https://doi.org/10.3329/icpj.v1i9.11613

Coopoosamy, R.M. and Magwa, M.L. (2006). Antibacterial activity of chrysophanol isolated from Aloe excelsa. African Journal of Biotechnology, *5*(16). 1508-1510.

Cuauthemone Sesquiterpenes and Flavones From Laggera Tomentosa Endemic TO ETHIOPIA. (2010). *Bulletin of the Chemical Society of Ethiopia, 24*(2), 267-271.

Debella, A., Kunert, O., Schmid, M.G., Michl, G., Bucar, F., Abebe, D.S., & Haslinger, E. (2000). A Diterpene, a Flavonol Glycoside, and a Phytosterol Glycoside from Securidaca longipedunculata and Entada abyssinica. *ChemInform, 131*, 401-408.

Declercq, J.P., Evrard, C., Clippe, A., Stricht, D.V., Bernard, A., & Knoops, B. (2001). Crystal structure of human peroxiredoxin 5, a novel type of mammalian peroxiredoxin at 1.5 A resolution. *J Mol Biol, 311*(4), 751-759. https://doi.org/10.1006/jmbi.2001.4853

Dibwe, D.F., Awale, S., Kadota, S., Morita, H., & Tezuka, Y. (2013). Heptaoxygenated xanthones as anti-austerity agents from Securidaca longepedunculata. *Bioorg Med Chem, 21*(24), 7663-7668. https://doi.org/10.1016/j.bmc.2013.10.027

El-Etrawy, A.-A.S., & Sherbiny, F. F. (2021). Design, synthesis, biological assessment and molecular docking studies of some new 2-Thioxo-2,3-dihydropyrimidin-4(1H)-ones as

potential anticancer and antibacterial agents. *Journal of Molecular Structure, 1225*, 129014. https://doi.org/10.1016/j.molstruc.2020.129014

Fekade, B. (2008). Phytochemical investigation of the pods of Senna occidentalis. [Master Thesis, AAU, Addis Ababa, Ethiopia].

Garg, A., Tadesse, A., & Eswaramoorthy, R. (2021). A Four-Component Domino Reaction: An Eco-Compatible and Highly Efficient Construction of 1,8-Naphthyridine Derivatives, Their In Silico Molecular Docking, Drug Likeness, ADME, and Toxicity Studies. *Journal of Chemistry, 2021*, 5589837. https://doi.org/10.1155/2021/5589837

Ghasemi, K., Ghasemi, Y., & Ebrahimzadeh, M. A. (2009). Antioxidant activity, phenol and flavonoid contents of 13 citrus species peels and tissues. *Pak J Pharm Sci, 22*(3), 277-281.

Gülçin, İ., Huyut, Z., Elmastaş, M., & Aboul-Enein, H.Y. (2010). Radical scavenging and antioxidant activity of tannic acid. *Arabian Journal of Chemistry, 3*(1), 43-53. https://doi.org/10.1016/j.arabjc.2009.12.008

Guo, S., Feng, B., Zhu, R., Ma, J., & Wang, W. (2011). Preparative isolation of three anthraquinones from Rumex japonicus by high-speed counter-current chromatography. *Molecules, 16*(2), 1201-1210. https://doi.org/10.3390/molecules16021201

Hakim, A., Akssira, M., Mina, L., Idrissi Hassani, L. M., Chebli, B., Hakmoui, A., . . . Blázquez, M. (2008). Chemical composition and antifungal activity of Bubonium imbricatum volatile oil. *Phytopathologia Mediterranea, 47*(1), 3-10. https://doi.org/10.14601/Phytopathol_Mediterr-2541

Joshi, R.K. (2013). Chemical constituents and antibacterial property of the essential oil of the roots of Cyathocline purpurea. *J Ethnopharmacol, 145*(2), 621-625. https://doi.org/10.1016/j.jep.2012.11.045

Lipinski, C.A., Lombardo, F., Dominy, B.W., & Feeney, P.J. (2001). Experimental and computational approaches to estimate solubility and permeability in drug discovery and development settings. *Adv Drug Deliv Rev, 46*(1-3), 3-26. https://doi.org/10.1016/s0169-409x(00)00129-0

Martin, N., Jirovetz, L., Buchbauer, G., & Fleischhacker, W. (2000). Investigation of the Essential Oil and Headspace of Laggera pterodonta (DC.) Sch. Bip. ex Oliv., a Medicinal Plant from Cameroon. *The Journal of Essential Oil Research, 12*, 345-349. https://doi.org/10.1080/10412905.2000.9699532

Mongalo, N.I., McGaw, L.J., Finnie, J.F., & Staden, J.V. (2015). Securidaca longipedunculata Fresen (Polygalaceae): a review of its ethnomedicinal uses, phytochemistry, pharmacological properties and toxicology. *J Ethnopharmacol, 165*, 215-226. https://doi.org/10.1016/j.jep.2015.02.041

Muto, A., Hori, M., Sasaki, Y., Saitoh, A., Yasuda, I., Maekawa, T., . . . Yoshida, T. (2007). Emodin has a cytotoxic activity against human multiple myeloma as a Janus-activated kinase 2 inhibitor. *Mol Cancer Ther, 6*(3), 987-994. https://doi.org/10.1158/1535-7163.Mct-06-0605

Nagatsu, A. (2004). Investigation of Anti-oxidative Compounds from Oil Plant Seed, Fabad J. Pharm. Sci., *29*, 203–210.

Ndukwe, K., Okeke, I., Lamikanra, A., Adesina, S., & Aboderin, O. (2005). Antibacterial Activity of Aqueous Extracts of Selected Chewing Sticks. *The journal of contemporary dental practice, 6*, 86-94. https://doi.org/10.5005/jcdp-6-3-86

Ołdak, A., Zielińska, D., Rzepkowska, A., & Kołożyn-Krajewska, D. (2017). Comparison of Antibacterial Activity of Lactobacillus plantarum Strains Isolated from Two Different Kinds of Regional Cheeses from Poland: Oscypek and Korycinski Cheese. *Biomed Res Int, 2017*, 6820369. https://doi.org/10.1155/2017/6820369

Omoregie, H., Okwute, & Koma, S. (2014). Some Bioactive Fatty Derivatives from *L. pterodonta*. *Nature and Science, 12*(1), 79-86.

Owolabi, M.S., Lajide, L., Villanueva, H.E., & Setzer, W.N. (2010). Essential oil composition and insecticidal activity of Blumea perrottetiana growing in southwestern Nigeria. *Nat Prod Commun, 5*(7), 1135-1138.

Panda, S., Jafri, M., Kar, A., & Meheta, B.K. (2009). Thyroid inhibitory, antiperoxidative and hypoglycemic effects of stigmasterol isolated from Butea monosperma. *Fitoterapia, 80*(2), 123-126. https://doi.org/10.1016/j.fitote.2008.12.002

Popelier, P.L.A. (2000). Atoms in Molecules: An Introduction; Pearson Education.

Qusti, S.Y., Abo-khatwa, A.N., Lahwa, M.A.B., & Qusti, S.Y. (2010). Screening of antioxidant activity and phenolic content of selected food items cited in the holly Quran. *EJBS*, *2*(1), 40–52

Rawat, D., Rawat, M. s. M., Semalty, A., & Semalty, M. (2013). Crysophanol-Phospholipid Complex: A Drug Delivery Strategy in Herbal Novel Drug Delivery System-HNDDS. *Journal of Thermal Analysis and Calorimetry, 111*, 2069-2077. https://doi.org/10.1007/s10973-012-2448-6

Tamano, M., & Koketsu, J. (1982). Isolation of Hydroxyanthrones from the Roots of Rumex acetosa Linn. *Agricultural and Biological Chemistry, 46*(7), 1913-1914. https://doi.org/10.1080/00021369.1982.10865350

Trott, O., & Olson, A.J. (2010). AutoDock Vina: improving the speed and accuracy of docking with a new scoring function, efficient optimization, and multithreading. *J Comput Chem, 31*(2), 455-461. https://doi.org/10.1002/jcc.21334

Verma, R., Padalia, R., Chanotiya, C., Chauhan, A., & Yadav, A. (2011). Chemical investigation of the essential oil of Laggera crispata (Vahl) Hepper & Wood from India. *J. Serb. Chem. Soc., 76*, 523–528. https://doi.org/10.2298/JSC100801048V

Vujovic, M., Ragavendran, V., Arsic, B., Kostic, E., & Mladenović, M. (2020). DFT calculations as an efficient tool for prediction of Raman and infra-red spectra and activities of newly synthesized cathinones. *Open Chemistry, 18*, 185-195. https://doi.org/10.1515/chem-2020-0021

Yamashita, S., Igarashi, M., Hayashi, C., Shitara, T., Nomoto, A., Mizote, T., & Shibasaki, M. (2015). Identification of self-growth-inhibiting compounds lauric acid and 7-(Z)-tetradecenoic acid from Helicobacter pylori. *Microbiology (Reading), 161*(6), 1231-1239. https://doi.org/10.1099/mic.0.000077